2017 21st International Conference on Process Control (PC)
June 6–9, 2017, Štrbské Pleso, Slovakia

Robust PID Controller Design for the Magnetic Levitation System: Frequency Domain Approach

Mária Hypiusová and Alena Kozáková
Institute of Automotive Mechatronics
Faculty of Electrical Engineering and Information Technology
Slovak University of Technology in Bratislava, Slovak Republic
maria.hypiusova@stuba.sk, alena.kozakova@stuba.sk

Abstract — **The paper deals with the frequency domain design of a robust PID controller for unstable SISO systems. The approach applied is based on performance specification in terms of phase and gain margins; to guarantee the desired performance a modification of the Neimark D-partition is used. In the case study a PID controller has been designed for the laboratory Magnetic Levitation System.**

Keywords*— *Robust PID controller, unstable system, D-partition, phase margin, Magnetic Levitation (maglev)

I. Introduction

In many real processes a controller has to cope with the effect of uncertainties that very often cause poor closed-loop performance or even instability. The reason for that are the perpetual changes of plant parameters (due to aging, influence of environment, working point changes *etc.*), as well as the unmodelled dynamics; the corresponding uncertainty description types are denoted parametric and dynamic uncertainty, respectively. A controller ensuring closed-loop stability under both of these uncertainty types is called robust controller. Many robust controller design methods are known from the literature [1 - 3] in both the frequency and time domains.

From the point of view of control engineering, magnetic levitation (maglev) systems are challenging due to nonlinear plant dynamics, a very small degree of natural damping in the process, strict positioning specifications often required by the application, and unstable dynamics.

Maglev technology has a wide range of applications, e.g. high-speed transportation systems [4], haptic interfaces [5], self-bearing blood pumps [6] for the use in artificial hearts, seismic attenuators for gravitational wave antennas [7], photolithography devices for semiconductor manufacturing [8] and microrobots [9].

Several methods for the gain and phase margin design technique for the first-order and second order plus time delay time plant models are proposed by [10 - 13].

In this paper, a graphical PID design approach for the maglev system based on the D-partition method [14] is presented. Usually, controllers guaranteeing desired phase margin are designed using Bode diagrams [10, 11]. In [17], the robust PID design for guaranteed phase margin was developed for the maglev system from Humusoft [18]; in this paper this approach was extended to design PID guaranteeing the prescribed gain and/or phase margins using the D-partition method, and applied to the laboratory maglev system by INTECO [15]. The design is applied for the nominal model, robust stability is verified using the robust stability condition for inverse additive uncertainty.

II. Robust PID controller Design for Desired Phase / Gain Margin

Consider the closed-loop feedback system shown in Fig. 1, where G_R(s) and $G_P(s)$ are transfer functions of the PID controller and the real plant, respectively; w, e, u and y are the reference, control error, manipulated variable and output of the plant, respectively.

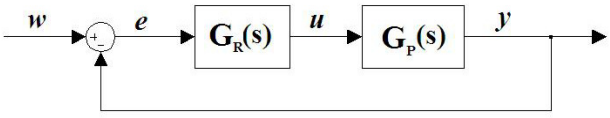

Fig. 1. Standard feedback system

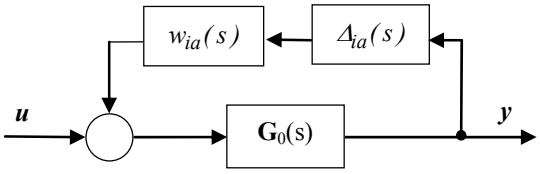

Fig. 2. Uncertain system modeled using inverse additive uncertainty

The uncertain plant will be modelled using unstructured uncertainty; as the plant is inherently unstable the inverse additive uncertainty is considered (Fig. 2).

$$G_p(s) = G_0(s)(I + w_{ia}(s)\Delta_{ia}(s)G_0(s))^{-1} \qquad (1)$$

where $G_0(s)$ is the nominal model; $w_{ia}(s)$ is a weighting stable transfer function ($|w_{ia}(j\omega)| \geq l_{ia}(\omega),\ \forall\omega$) and $\Delta_{ia}(s)$ is a normalized uncertainty ($\Delta_{ia}(s) \leq 1$).

For this uncertainty type it is possible to calculate the weighting function $l_{ia}(\omega)$ as follows:

$$l_{ia}(\omega) = \max_k \sigma_M (G_k(j\omega)^{-1} - G_0(j\omega)^{-1}) \tag{2}$$

The M-delta structure based robust stability condition [13] will be used in the following form

$$\sigma_M(M_0(s)) < \frac{1}{l_{ia}(\omega)} \tag{3}$$

where $M_0(s) = \dfrac{G_0(s)}{1 + G_R(s)G_0(s)}$ (4)

Condition (3) will be verified graphically.

The nominal model can be obtained e.g. from N identifications of the plant (in N working points) by taking mean values of the nominator and denominator coefficients, respectively:

$$G_0(s) = \frac{(B_1(s) + ... + B_N(s))/N}{(A_1(s) + ... + A_N(s))/N} \tag{5}$$

Consider the PID controller transfer functions

$$G_R(s) = k + \frac{k_i}{s} + k_d s \tag{6}$$

The problem studied in this paper can be formulated as follows: For the uncertain system $G_P(s)$ described by (1) a robust PID controller $G_R(s)$ is to be designed using the Neimark D-partition such that closed-loop stability and performance specified in terms of phase margin and / or gain margin is guaranteed. If the PID controller designed for the nominal plant satisfies condition (3), then closed-loop and of the uncertain plant described using unstructured additive uncertainty is ensured.

For nominal model the characteristic equation is

$$1 + G_R(s)G_0(s) = 0 \tag{7}$$

A small modification of (7) yields

$$k + \frac{k_i}{s} + k_d s = -\frac{A(s)}{B(s)} \tag{8}$$

Using substitution $s = j\omega$ it is possible to obtain real and imaginary parts of (8):

$$\begin{aligned} RE &: k = \mathrm{Re}\left\{-\frac{A(j\omega)}{B(j\omega)}\right\} \\ IM &: -\frac{k_i}{\omega} j + k_d j\omega = \mathrm{Im}\left\{-\frac{A(\omega)}{B(\omega)}\right\} \end{aligned} \tag{9}$$

By changing ω frequency-by-frequency within the interval $\omega \in (0, \infty)$ from the real part of (9) it is possible to calculate a frequency dependent vector of complex numbers which plotted in the complex plane gives the D-curve for the parameter k; similarly, from the imaginary part of (9) it is possible to obtain k_i or k_d, however not both at once. In one step it is possible to plot D-curve for the parameters k and k_i (PI controller) or k and k_d (PD controller).

Using a small modification of the characteristic equation we obtain

$$1 + G_R(s)G_0(s)\,GM\,e^{-j\,PM} = 0 \tag{10}$$

Thu, it is possible to move and rotate the Nyquist plot of a system, where GM is the gain margin and PM the phase margin (angle of desired rotation in radians). Then the D-curves calculated with (10) are

$$\begin{aligned} RE &: k = \mathrm{Re}\left\{-\frac{A(j\omega)}{B(j\omega)\,GM\,e^{-j\,PM}}\right\} \\ IM &: -\frac{k_i j}{\omega} + k_d j\omega = \mathrm{Im}\left\{-\frac{A(j\omega)}{B(j\omega)\,GM\,e^{-j\,PM}}\right\} \end{aligned} \tag{11}$$

Controller parameters can directly be chosen from the D-curves. The designed controller will ensure gain margin and phase margin. To meet design specification in terms of the gain margin GM we set $PM = 0$, and vice-versa for design specification in terms of the phase margin PM we set $GM = 0\,\mathrm{dB}$. In general, large values of GM and PM correspond to sluggish closed-loop responses while their smaller values result in less sluggish, more oscillatory responses. When GM and PM are large the system will be more robust.

The PID controller design consists of two steps: in the first step, a PD controller is designed, and in the second step a PI controller design is applied for the plant with the PD controller. Then, the PID controller is calculated as follows

$$G_R(s) = (k_1 + k_d s)(k_2 + \frac{k_i}{s}) =$$
$$= (k_1 k_2 + k_d k_i) + \frac{k_i k_1}{s} + k_d k_2 s = \quad (12)$$
$$= P + \frac{I}{s} + Ds$$

In this way it is possible to design a PID controller for the unstable plant if it is stabilizable by a PD controller. Hence, in the first step, a PD controller is used for stabilization and a PI controller guarantees the desired phase margin and eliminates steady state offset.

III. Magnetic Levitation System

Levitation [15] is a stable equilibrium of an object without contact and can be achieved using electric or magnetic forces. In a magnetic levitation, or maglev system a ferromagnetic object is suspended in air using electromagnetic forces. These forces cancel the effect of gravity, effectively levitating the object and achieving stable equilibrium.

The basic control task is to control position of the ball freely levitating in the magnetic field of the coil. The magnetic levitation system with 2 electromagnets is shown in Fig. 3.

Fig. 3. The magnetic levitation system from INTECO, Ltd.

We used only one electromagnet (the upper one). Using linearization of the nonlinear model [16] three working points for the medium ball have been chosen within the working range of the plant; they are defined by the vertical position of the ball $x\,[mm]$ and corresponding input voltage u_{10} [MU]:

WP1: $x = 8[mm]$ $u_{10} = 0{,}2658[MU]$

WP2: $x = 10[mm]$ $u_{10} = 0{,}2986[MU]$

WP3: $x = 12[mm]$ $u_{10} = 0{,}3375[MU]$

Corresponding transfer functions are as follows:

$$G_{p_1} = \frac{-2{,}0893.10^4}{s^3 + 186{,}2891 s^2 - 1{,}6847.10^3 s - 3{,}1384.10^5}$$
$$G_{p_2} = \frac{-2{,}7277.10^4}{s^3 + 288{,}7746 s^2 - 1{,}6847.10^3 s - 4{,}8649.10^5} \quad (15)$$
$$G_{p_3} = \frac{-3{,}5611.10^4}{s^3 + 447{,}6417 s^2 - 1{,}6847.10^3 s - 7{,}5413.10^5}$$

Each transfer function has one unstable real root:

$$G_{p_1}: \quad -186{,}3; \quad -41{,}045; \quad 41{,}045$$
$$G_{p_2}: \quad -288{,}8; \quad -41{,}045; \quad 41{,}045$$
$$G_{p_3}: \quad -447{,}6; \quad -41{,}045; \quad 41{,}045$$

IV. Robust PID Controller Design for the Magnetic Levitation System

The robust PID controller design procedure was applied for the nominal model obtained according to (5)

$$G_0(s) = \frac{-2{,}7927.10^4}{s^3 + 307{,}6 s^2 - 1{,}685.10^3 s - 5{,}182.10^5} \quad (16)$$

The $k_1 - k_d$ D-curves for the specified $GM = 5[dB]$ and $PM = 45^\circ$ have been calculated and are depicted in Fig. 4.

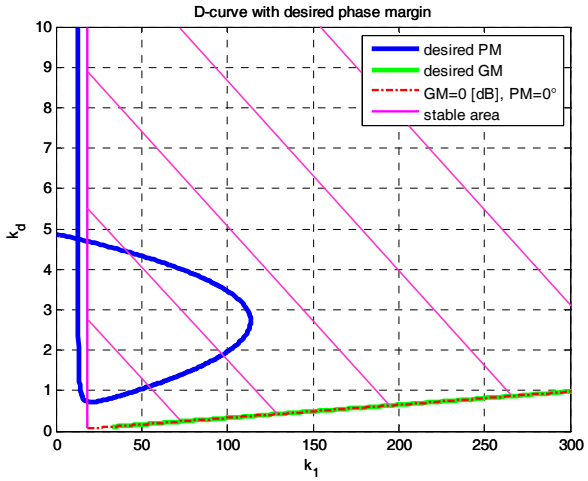

Fig. 4. D-curves for the parameters k_1 and k_d

In the first step we just wanted to stabilize the system, hence it was not necessary to choose parameters from the blue or green lines. The system is stable if controller parameters are chosen from the stable area (magenta). The magenta line represents the stability boundary. Following PD controller parameters were chosen:

$$k_1 = 40 \text{ and } k_d = 11.$$

Corresponding closed loop poles are

$$-152{,}8 \pm 530{,}63i \quad \text{and} \quad -1{,}96$$

In the second step, a PI controller is designed for the closed-loop system consisting of the plant and the designed PD controller. D-curves for k_2 and k_i have been calculated and are depicted in Fig. 5.

Controller parameters guaranteeing desired phase margin $PM = 45°$ and desired gain margin $GM = 5[dB]$ were chosen from the blue line in Fig. 5. Parameters of the designed PI controller have been read from the intersection of the curves of desired GM and PM, respectively: $k_2 = 0{,}412$ and $k_i = 1{,}526$. The final controller calculated according (12) is:

$$G_R(s) = 33{,}27 + \frac{61{,}04}{s} + 4{,}532s \qquad (17)$$

Using the second point of intersection of the desired GM and PM curves in Fig. 5 yields controller parameters $k_2 = 0{,}0803$ and $k_i = 2{,}986$; closed-loop simulation results under the controller calculated according to (12) show very fast dynamics (settling time 0.48s), however when the controller is implemented the real closed-loop plant is unstable.

Bode plots showing that the desired gain and phase margins were achieved are depicted in Fig. 6.

Closed-loop poles under the designed PID controller are:

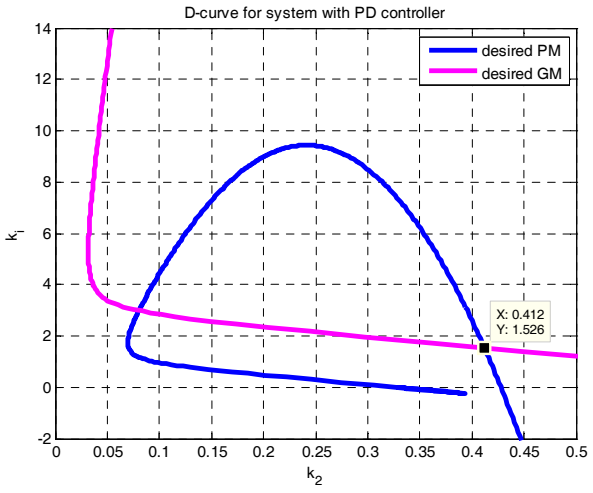

Fig. 5. D-curve in the $k_2 - k_i$ plane

$$-152{,}14 \pm 317{,}36i \quad \text{and} \quad -1{,}64 \pm 3{,}33i$$

Verification of the condition (3) in Fig. 7 shows that closed-loop robust stability has been achieved.

If the closed-loop under the designed controller does not meet the robust stability condition it is necessary to increase the desired gain and phase margins and repeat the controller design.

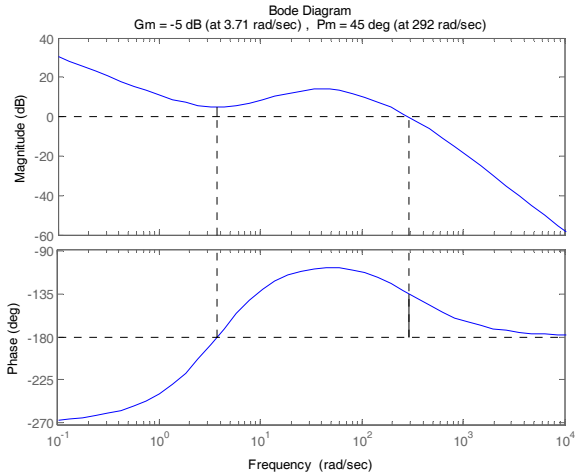

Fig. 6. Bode plots of the magnetic levitation plant under the designed PID controller

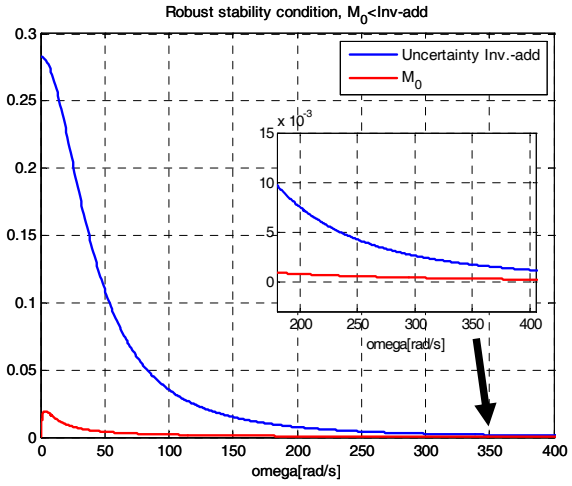

Fig. 7. Verification of the robust stability condition

Controller parameters calculated for various selected gain and phase margins are shown in the below Table I and Table II.

To guarantee performance specified in terms of GM, we can choose any point on the GM D-curve, and similarly for a specified PM, any point on the PM D-curve can be chosen.

The results of experiments on the real plant with the robust controller designed for GM=5 [dB] and various PM are in Fig. 8, 9 and 10. Experimental results with the robust controller designed for PM=40 [°] and various GM are depicted in Fig.

TABLE I. PARAMETER VALUES FOR VARIOUS GAIN MARGIN (*GM*) AND PHASE MARGIN (*PM*)

	***Desired GM* [dB]**	***Desired PM* [°]**	k_1	k_d	k_2	k_i
1	5	45	40	11	0,412	1,526
2	5	40	50	20	0,3029	0,9001
3	5	35	20	10	0,8234	1,661
4	5	30	20	20	0,5775	1,074
5	10	40	100	20	0,2896	1,534
6	8	40	25	6	0,9869	3,731
7	-	40	25	6	0,9679	5,653
8	5	-	20	5	0,8044	3,45

TABLE II. PID CONTROLLERS DESIGNED FOR VARIOUS DESIRED GAIN MARGINS (*GM*) AND PHASE MARGINS (*PM*)

	$G_R(s)$
1	$33{,}27+\frac{61{,}04}{s}+4{,}532s$
2	$33{,}15+\frac{45{,}01}{s}+6{,}058s$
3	$33{,}08+\frac{33{,}22}{s}+8{,}234s$
4	$33{,}03+\frac{21{,}48}{s}+11{,}55s$
5	$59{,}64+\frac{153{,}4}{s}+5{,}792s$
6	$47{,}06+\frac{93{,}27}{s}+5{,}921s$
7	$58{,}12+\frac{141{,}3}{s}+5{,}807s$
8	$33{,}34+\frac{69}{s}+4{,}022s$

11, 12 and 13 show. Step responses were performed in the three working points.

Based on performance assessment in terms of maximum overshoot and settling time we can conclude that for a constant *GM*, the settling time decreases with increasing *PM* and for a constant *PM*, the settling time decreases with increasing *GM*; the trade-off between the settling time and the overshoot is evident. From closed-loop simulation, *GM* = 9,8 [dB] is obtained for 7th controller, and *PM* = 47,1 [°] for 8th controller.

V. CONCLUSION

In this paper a modification of the standard Neimark D-partition method was applied to design robust PID controllers for the unstable Magnetic Levitation Model. This controller design approach guarantees not only closed-loop stability but also performance in terms of gain and / or phase margins. The proposed frequency domain design method is graphical, interactive and insightful, and is applicable for both stable and unstable systems.

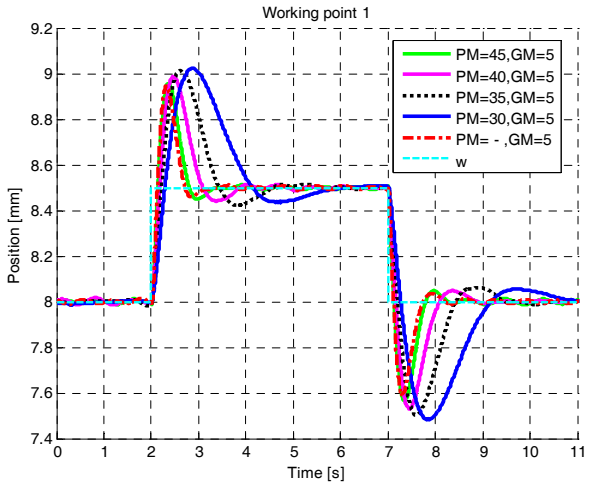

Fig. 8. Step responses for *GM* = 5 [dB] in the 1st working point

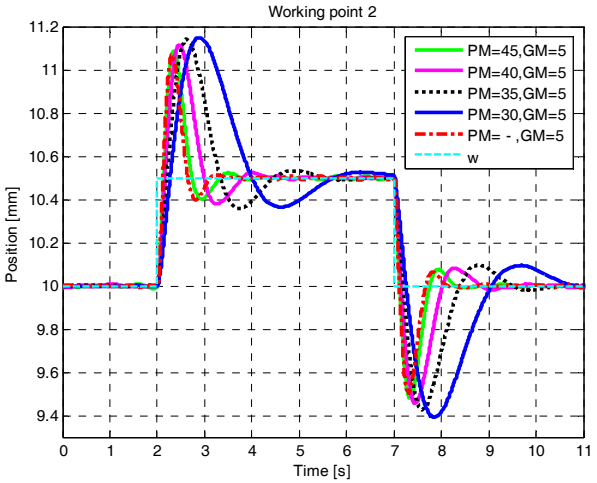

Fig. 9. Step responses for *GM* = 5 [dB] in the 2nd working point

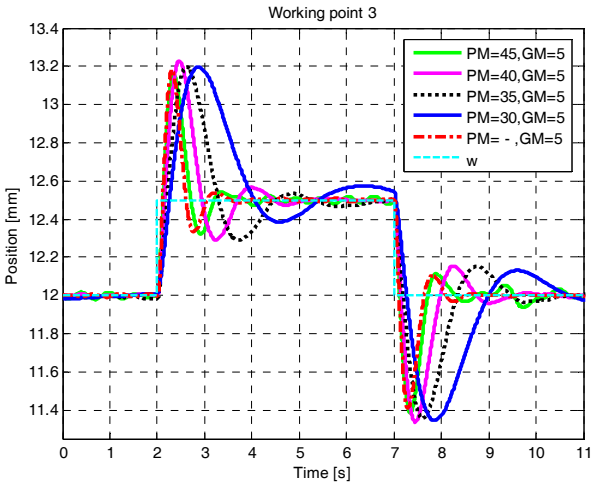

Fig. 10. Step responses for *GM* = 5 [dB] in the 3rd working point

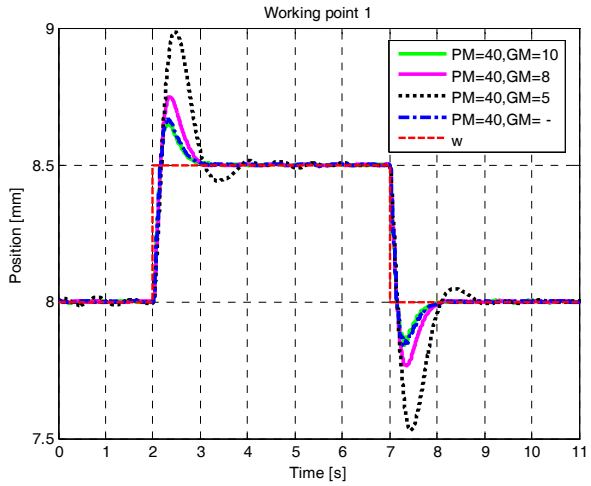

Fig. 11. Step responses for $PM = 40$ [°]in the 1st working point

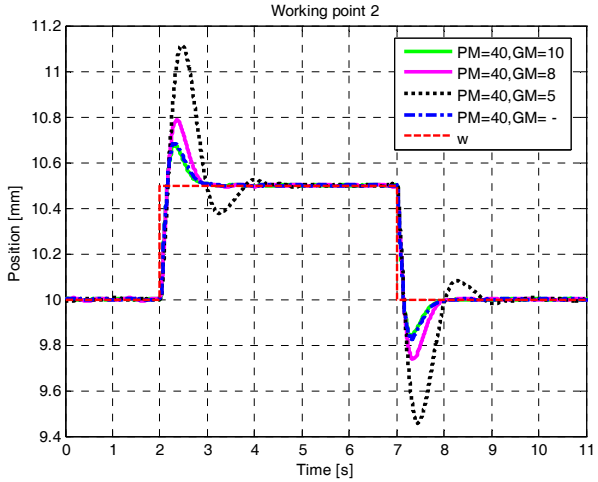

Fig. 12. Step responses for $PM = 40$ [°] in the 2nd working point

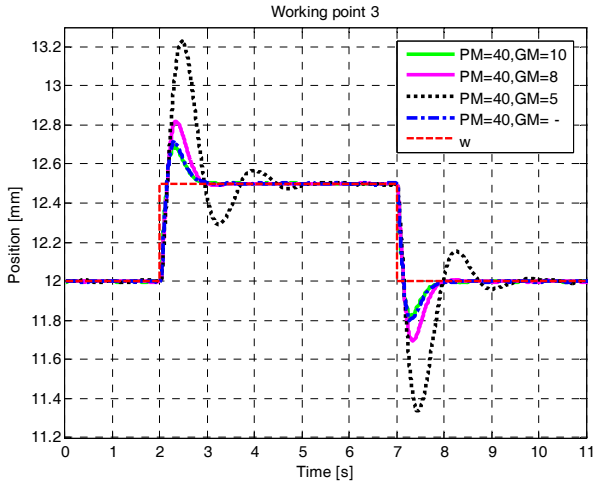

Fig. 13. Step responses for $PM = 40$ [°] in the 3rd working point

ACKNOWLEDGMENT

This work has been supported by the Scientific Grant Agency of the Ministry of Education, Science, Research and Sport of the Slovak Republic under Grant No. 1/0733/16, and by the SRDA grant APVV-0772-12.

REFERENCES

[1] J. Ackerman. Robust Control – Systems with Uncertain Physical Parameters. Springer-Verlag London Limited, 406s. ISBN 0-387-19843-1, 1997.

[2] S. P. Bhattacharyya, H. Chapellat and L. H. Keel, Robust Control: The parametric Approach. Prentice Hall, 647 s. ISBN 0-13-781576-X, 1995.

[3] S. Skogestad, I. Postletwaite: Multivariable feedback control: analysis and design, John Wiley & Sons, 1996.

[4] P. Holmer: Faster than a speeding bullet train, IEEE Spectrum, Vol. 40, No. 8, pp. 30-34, 2003.

[5] P.J. Berkelman and R.L. Hollis: Lorentz magnetic levitation for haptic interaction: Device design, performance, and integration with physical simulations, International Journal of Robotics Research, Vol. 19, No. 7, pp. 644-667, 2000.

[6] T. Masuzawa, S. Ezoe, T. Kato, Y. Okada: Magnetically suspended centrifugal blood pump with an axially levitated motor, Artificial Organs, Vol. 27, No. 7. pp. 631-638, 2003.

[7] M. Varvella, E. Calloni, L. Di Fiore, L. Milano and N. Arnaud: Feasibility of magnetic suspension for second generation gravitational wave interferometers, Astroparticle Physics, Vol. 21, No. 3, pp. 325-335, 2004.

[8] W.J. Kim And D.L. Trumper: High-precision magnetic levitation stage for photolithography, Precision Engineering, Vol. 22, No. 2, pp. 66-77, 1998.

[9] M.B. Khamesee, N. Kato, Y. Nomura and T. Nakamura: Design and control of a microrobotic system using magnetic levitation, EEE-ASME Transactions on Mechatronics, Vol. 7, No. 1, pp. 1-14, 2002.

[10] H.W. Fung, Q.G. Wang, T.H. Lee: PI Tuning in terms of gain and phase margins, Automatica, 34, pp. 1145-1149, 1998.

[11] W.K. Ho, C.C. Hang, L. Cao: Tuning of PID controllers based on gain and phase margin specifications, Automatica, 31, pp. 497-502, 1995.

[12] O. Yaniv, M. Nagurka: Design of PID controllers satisfuing gain margin and sensitivity constraints on a set of plants, Automatica, Vol. 40, pp. 111-116, 2004.

[13] N. M. Darwish: Design of robust PID controllers for first-order plus time delay systems based on frequency domain specifications, Journal of Engineering Sciences Assiut University, Egypt, vol. 43, No. 4, pp. 472-489, 2015.

[14] Y.I. Neimark: Robust stability and D-partition, Automation and Remote Control 53 (7), pp. 957–965, 1992.

[15] INTECO Ltd, Magnetic Levitation System 2EM (MLS2EM), User's Manual, Krakow, Poland, 2008.

[16] P. Balko, D. Rosinová: Modeling of magnetic levitation system. Submitted to 21st International Conference on Process Control, Štrbské Pleso, Slovakia, June 2017.

[17] M. Hypiusová, J. Osuský: Robust controller design for magnetic levitation model, AT&P Journal Plus: Systems of automatic control, num 1, 2010, pp 100-104.

[18] CE 152 Magnetic levitation model – education manual. *Humusoft s.r.o.* 2002.